J. Great Lakes Res. 34:721–730
Internat. Assoc. Great Lakes Res., 2008

Tracking the Surface Flow in Lake Champlain

Michael J. McCormick[1], Thomas O. Manley[2], Dmitry Beletsky[3,*], Andrew J. Foley III[3,†], and Gary L. Fahnenstiel[4]

[1]*19150 Sibley Road*
Chelsea, Michigan 48118

[2]*Middlebury College*
Middlebury, Vermont 05753

[3]*CILER, SNRE*
University of Michigan
Ann Arbor, Michigan 48105

[4]*NOAA GLERL*
Lake Michigan Field Station
Muskegon, Michigan 49441

ABSTRACT. *Understanding the hydrodynamics of Lake Champlain is a basic requirement for developing forecasting tools to address the lake's environmental issues. In 2003 through 2005, surface drifting buoys were used to help characterize the circulation of the main body and northeast region (Inland Sea) of the lake. Progressive vector diagrams of over-lake winds when compared to drifter trajectories suggest the presence of gyre-like circulation patterns. Drifter statistics suggest average current speeds of 10 cm* s^{-1} *and were predominantly northward (+ V) due to northerly-directed winds and lake geometry. Single-particle eddy diffusivities on the order of* 10^6 cm^2 s^{-1} *were calculated which is consistent with results from the Great Lakes and in some oceanic regions. However, the Lagrangian length and time scales, a measure of flow decorrelation scales, were in general smaller than seen in the Great Lakes, which is a natural consequence of the smaller basin size of Lake Champlain relative to the Great Lakes.*

INDEX WORDS: *Surface drifters, Lagrangian statistics, Lake Champlain.*

INTRODUCTION

Lake Champlain lies in the valley between the Green Mountains of Vermont to the east, the Adirondack Mountains of New York to the west, and the Canadian province of Quebec to the north. Following the Great Lakes it is the sixth largest lake in the United States, and like the rest of the Great Lakes is confronted with similar problems. Current issues range from mercury contamination from atmospheric deposition, cultural eutrophication, aquatic invasive species, harmful algal blooms, critical habitat loss for fish and wildlife, drinking water quality, and protecting submerged cultural resources.

The lake is primarily oriented in an N-S direction extending 193 km with the widest section occurring in the main body of the lake, spanning 19 km (Fig. 1). The bathymetry of Lake Champlain is characterized by steep gradients with a maximum depth of 122 m and a mean of 19.5 m. A natural consequence of the basin geometry is internal seiching and gravity currents or bores along the thermocline when the water column is vertically stratified. Observations suggest that internal seiching persists throughout the stratified season with often large, nonlinear, asymmetrical, internal waves of 10 m to nearly 60 m in height (Manley *et al.* 1999, Saylor *et al.* 1999).

Understanding the hydrodynamics of Lake Champlain is a basic requirement for developing forecasting tools to address most of the lake's environmental issues. A set of relatively extensive measurements of the subsurface current and thermal

*Corresponding author. E-mail: dima.beletsky@noaa.gov
†Current address: Earth Tech AECOM, Alexandria, VA 22314

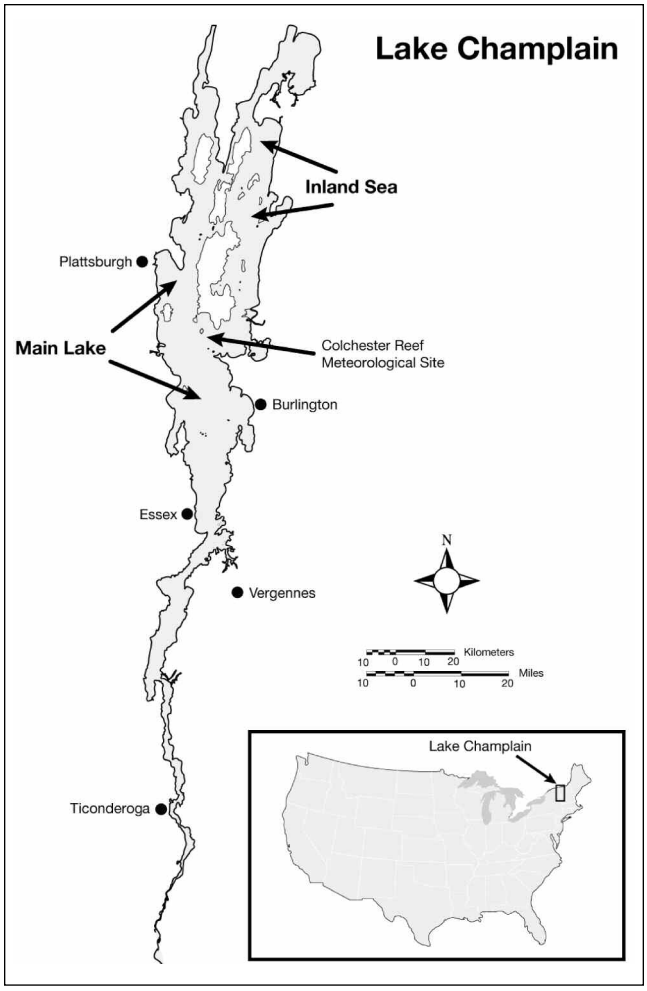

FIG. 1. Lake Champlain with the main lake and the Inland Sea identified.

structure have been made in the main body of the lake with very limited observations in the southern portion and northeast region of Lake Champlain. Even fewer observations of the surface currents exist. McCormick *et al.* (2006) describes Lagrangian observations of the surface currents from 2003 made by satellite-reporting drifting buoys in the main body of the lake. In this paper we include Lagrangian measurements from 2004 conducted in the main body of the lake and also 2005 data where drifting buoys tracked the surface flow in the northeast portion of Lake Champlain.

METHODS

Satellite-reporting drifting buoys made by Clearwater Instrumentation (ClearSat GPS/ARGOS buoy) were used exclusively to track the surface circulation in Lake Champlain. These are CODE (Coastal Ocean Dynamics Experiment) type drifters with excellent water tracking capability because of very low direct wind- and wave-induced horizontal motion to the drifter (Davis 1985). The drifter consists of a 1-m-long tube that houses the electronics and battery pack. Attached to the housing are four drogue/vanes directed radially outward at 90° intervals with a small surface float attached at the outward end of each vane. The drifter has a center-of-effort at approximately 0.8 m below the water surface. The drifters are equipped with both GPS and ARGOS positioning capability. The low resolution ARGOS positions are determined by Doppler shifting with a maximum accuracy of 150 m. The GPS positions are much more accurate than ARGOS and are measured once every hour. A maximum of 17 GPS positions may be stored in the drifter's on-board microprocessor and transmitted to satellite, processed by ARGOS, and made available to the end-user in near real time. The small data transmission window for ARGOS requires that the GPS data be highly compressed and encoded to minimize the chances of losing any positioning data. Only GPS data were used in the analyses because of the combination of lower accuracy and less frequent positions of ARGOS compared to GPS.

In contrast to typical oceanic applications, all drifters were retrieved rather than treated as expendable. Drifter tracks were regularly monitored, and once a drifter appeared to be entering shoal water, a boat was used at the earliest opportunity to locate and retrieve the buoy before it suffered serious damage. To speed up the recovery operation, a pulse direction finder (IESM-GONIO 400 P) was used to hone in on the ARGOS transmissions. Once a drifter was recovered, it was frequently redeployed and the entire process repeated throughout the duration of the experiment.

Meteorological data from 2004 were obtained from a meteorological site maintained on Colchester Reef located in the main body of Lake Champlain approximately 30 km NW of Burlington, Vermont (Fig. 1). The data were obtained from the Vermont Monitoring Cooperative and were used to model the drifter trajectories.

RESULTS AND DISCUSSION

Mean Speed, Velocity, Mean and Fluctuating Kinetic Energy

Each trajectory was divided into 1.0 h segments from which all of the statistics were calculated. The

velocity components (u, v) are orthogonal, with a right-handed convention used, with u, positive to the east (x axis), and v, positive to the north (y axis). The mean speed (S), mean velocity (U, V), and mean kinetic energy (MKE) were calculated according to:

$$S = \frac{1}{n}\sum_{i=1}^{n}\left(u_i^2 + v_i^2\right)^{\frac{1}{2}},\ U = \frac{1}{n}\sum_{i=1}^{n}u_i,\ V = \frac{1}{n}\sum_{i=1}^{n}v_i \qquad (1)$$

$$MKE = \frac{1}{2n}\sum_{i=1}^{n}\left(u_i^2 + v_i^2\right) \qquad (2)$$

where (u_i, v_i) are the ith velocity components, and n is the total number of time segments of an individual trajectory. All of the energy calculations described here are per unit mass.

Table 1 lists the drifter identification, their start and end dates, and their duration for 2003 through 2005. The 2003 data set is the smallest with four tracks used in the analyses. In 2003, several drifters were deployed across the main body of Lake Champlain westward from Burlington, Vermont. Only four of the tracks are reported here because of drifters running aground shortly after being deployed. Only tracks that were longer in time than one day are used. The tracks are shown in Figure 2.

Examining Table 1 and Figure 2, drifters numbered 2 and 4 produced Lagrangian data of less than 2 days duration, while the drifters released 2 days later (drifters 1 and 3) tracked the surface currents for several days before running aground. Drifters 2 and 4 traveled predominantly up the long axis of the lake compared to drifters 1 and 3 that experienced two flow reversals. Shortly after their deployment, drifters 1 and 3 traveled several kilometers southward until the flow reversed back again to the north, and both drifter trajectories were northward along the main axis of the lake. The predominant flow direction for the 2003 experiment was north. For 2003, the U component of the velocity was near zero, and the V component ranged from 4 to 9 cm s^{-1} (Table 2). The mean speeds of all the drifters were higher, ranging from a low of 9 to a high of 14 cm s^{-1}. When flow reversals are indicated by a drifter trajectory, the mean speed will

TABLE 1. Deployment dates for 2003–2005. Drifter ID's correspond to those shown in Figures 2–5.

Year	Drifter ID	Start Time Date (DOY)	End Time Date (DOY)	Duration (days)
2003	1	17 July (198.75)	25 July (206.50)	7.75
2003	2	15 July (196.63)	17 July (198.25)	1.63
2003	3	17 July (198.75)	22 July (203.63)	4.88
2003	4	15 July (196.69)	17 July (198.63)	1.94
2004	1	1 July (183.12)	4 July (186.42)	3.30
2004	2	8 Aug (221.77)	12 Aug (225.10)	3.33
2004	3	15 Aug (228.80)	17 Aug (230.83)	2.03
2004	4	14 July (196.75)	22 July (204.54)	7.79
2004	5	23 July (205.44)	25 July (207.60)	2.16
2004	6	3 Aug (216.88)	8 Aug (221.54)	4.66
2004	7	8 Aug (221.81)	11 Aug (224.23)	2.42
2004	8	14 July (196.75)	17 July (199.63)	2.88
2004	9	30 July (212.71)	3 Aug (216.38)	3.67
2004	A	8 Aug (221.81)	15 Aug (228.52)	6.71
2004	B	15 Aug (228.79)	17 Aug (230.79)	2.00
2004	C	28 June (180.75)	30 June (182.92)	2.17
2004	D	14 July (196.69)	22 July (204.31)	7.62
2004	E	8 Aug (221.81)	10 Aug (223.85)	2.04
2005	1	15 July (196.96)	18 July (199.08)	2.12
2005	2	15 July (196.96)	18 July (199.00)	2.04
2005	3	31 July (212.50)	3 Aug (215.75)	3.25
2005	4	5 Aug (217.75)	7 Aug (219.79)	2.04
2005	5	31 July (212.50)	5 Aug (217.00)	4.50
2005	6	5 Aug (217.88)	9 Aug (221.92)	4.04

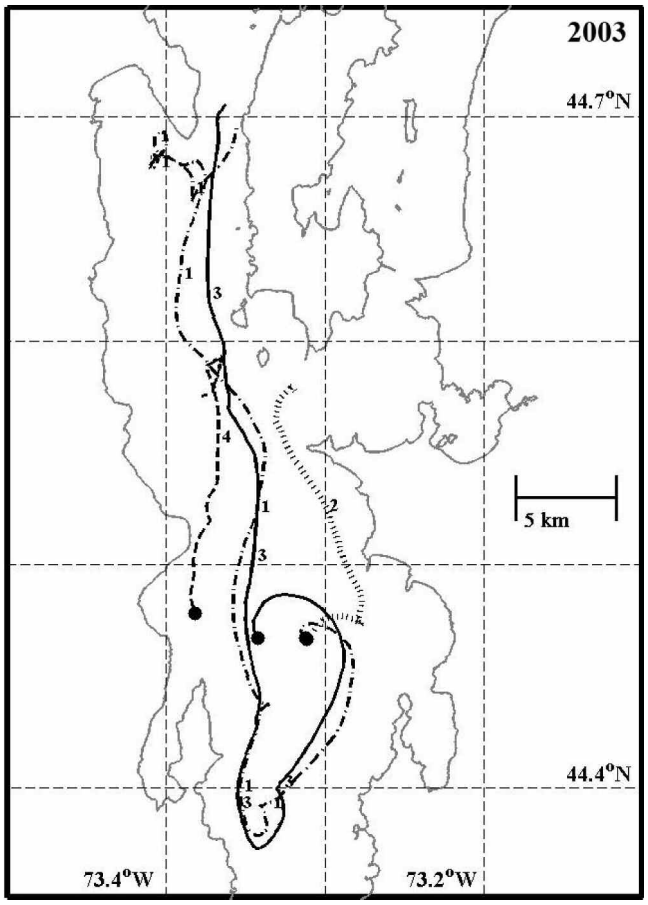

FIG. 2. Drifter tracks for 2003. Line styles for individual drifter tracks are: 1(-.), 2(=), 3(—), and 4(--). All tracks begin at the dark circles, and track symbols repeat every 24 h. Drifters 1 and 2 start very close to the same location.

always be greater than or equal to the mean velocity because of the nature of the averaging process as seen in Eq. 1.

The *MKE*, as expected, was well correlated with the mean drifter speeds with the highest *MKE* of 117 $cm^2\ s^{-2}$ associated with drifter 3, which also had the highest mean speed. Drifters 1, 2, and 4 had *MKE* values (58–88 $cm^2\ s^{-2}$) that were comparable to that of the overall *MKE* for all three years of 68 $cm^2\ s^{-2}$ (Table 2).

Strong stratification inhibits vertical mixing of surface and bottom waters and may directly impact the water quality. There is much literature (e.g., Martin 1985, McCormick and Meadows 1988) describing approaches toward parameterizing vertical mixing ranging from shear induced instabilities, turbulence kinetic energy, and fickian diffusion. All involve either the horizontal currents or their fluctuating components or combinations thereof, in some critical stability parameter, e. g., Gradient Richardson Number or Froude Number, and/or parameterize the Reynolds stresses to estimate vertical mixing. Estimates of the fluctuating kinetic energy (*FKE*) is yet another approach and it too may provide insights on flow variability and energy availability for vertical mixing. The *FKE* was estimated by

$$FKE = \frac{1}{n}\sum_{i=1}^{n}(s_i - S)^2,\ s_i = \left(u_i^2 + v_i^2\right)^{\frac{1}{2}} \qquad (3)$$

where s_i is the i^{th} speed calculation of the time series of length n, and S is a suitable time average. Some authors (Rao and Murthy 2001) have used data that were low-passed filtered with all frequencies with periods of less than 24 h removed. The S in Eq. 3 is then replaced by the low-passed filtered data. Given the relatively short length of these drifter tracks, we chose to use the mean speed (Eq. 1) of each track to estimate S. For 2003, the *FKE* was much less than the *MKE*, ranging from 13 to 26 $cm^2\ s^{-2}$. In general, the *FKE* was significantly less than the *MKE* throughout all years (Table 2).

A total of 14 drifter tracks were recorded in 2004. All deployments were in the main body of Lake Champlain. Figure 3a shows all of the tracks, while in Figures 3b–d, the tracks are sorted for greater clarity. In general, all trajectories were dominated by a northerly component (+ *V*) with the largest *V* seen in drifters 1 and 8 (Table 2). Drifter 1 progressed the furthest north of any drifter, while drifter 6 was the only drifter to have a *U* component larger than the *V* component. In the later case, drifter 6 began traveling south until the flow field reversed direction and then it headed north, paralleling the initial trajectory but displaced to the west, resulting in a net transport to the west. The *MKE* of the 2004 data ranged from a low of 41 $cm^2\ s^{-2}$ to a high of 156 $cm^2\ s^{-2}$, while the *FKE* showed a much greater relative range of 6 to 78 $cm^2\ s^{-2}$ (Table 2).

In 2005, the Lagrangian experiments were moved from the main body of Lake Champlain to the northeast region called the Inland Sea (Manley *et al.* 1999). The Inland Sea is characterized by shallow water with islands and embayments throughout the region often resulting in short duration drifter excursions because of the drifters running aground. Nonetheless, a total of six drifter tracks were of sufficient duration (Table 2) to be used in the analyses (Fig. 4.).

The results for 2005 were comparable to the ex-

TABLE 2. Lagrangian statistics for drifter experiments conducted in 2003–2005 in Lake Champlain.

			Mean S, U, V (cm s^{-1})			MKE & FKE		Lagrangian Time & Length				Eddy Diff. × 10^6	
Yr	ID	Dur. (h)	S	U	V	(cm^2 s^{-2})		T_x (h)	T_y (h)	L_x (km)	L_y (km)	K_x (cm^2 s^{-1})	K_y (cm^2 s^{-1})
’03	1	186	10	–1	4	75	26	4	16	0.7	6.1	0.38	6.3
’03	2	39	12	0	9	88	20	4	12	1.0	3.1	0.71	2.2
’03	3	117	14	0	6	117	26	3	17	0.7	8.0	0.37	10.0
’03	4	46	9	0	6	58	13	1	11	0.1	3.0	0.04	2.4
’04	*1*	*79*	*13*	*0*	*9*	*156*	*78*	*2*	*11*	*0.3*	*5.5*	*0.14*	*7.8*
’04	*2*	*80*	*9*	*1*	*5*	*54*	*16*	*5*	*13*	*1.0*	*3.4*	*0.47*	*2.6*
’04	*3*	*49*	*8*	*2*	*5*	*42*	*7*	*8*	*12*	*1.1*	*2.6*	*0.45*	*1.5*
’04	*4*	*187*	*10*	*0*	*5*	*80*	*28*	*3*	*16*	*0.5*	*5.8*	*0.24*	*6.1*
’04	*5*	*52*	*10*	*–2*	*5*	*80*	*29*	*3*	*6*	*0.7*	*2.3*	*0.38*	*2.2*
’04	*6*	*112*	*9*	*–1*	*0*	*60*	*20*	*2*	*7*	*0.4*	*2.5*	*0.17*	*2.5*
’04	*7*	*58*	*10*	*2*	*5*	*70*	*16*	*4*	*8*	*0.7*	*2.7*	*0.37*	*2.5*
’04	*8*	*69*	*11*	*–2*	*7*	*97*	*31*	*6*	*14*	*1.3*	*4.9*	*0.82*	*4.7*
’04	*9*	*88*	*10*	*1*	*2*	*66*	*13*	*1*	*4*	*0.2*	*1.2*	*0.13*	*1.2*
’04	*A*	*161*	*8*	*–1*	*2*	*47*	*13*	*3*	*7*	*0.7*	*1.9*	*0.44*	*1.4*
’04	*B*	*48*	*8*	*3*	*5*	*42*	*7*	*7*	*12*	*1.2*	*2.5*	*0.47*	*1.5*
’04	*C*	*52*	*8*	*0*	*5*	*41*	*6*	*3*	*11*	*0.5*	*2.3*	*0.26*	*1.4*
’04	*D*	*183*	*11*	*0*	*5*	*91*	*33*	*3*	*15*	*0.5*	*6.1*	*0.27*	*7.0*
’04	*E*	*49*	*10*	*3*	*7*	*73*	*18*	*6*	*10*	*1.0*	*3.0*	*0.45*	*2.6*
’05	1	51	8	2	3	44	10	6	8	1.3	1.6	0.80	1.0
’05	2	49	9	3	4	60	15	7	8	1.5	2.1	0.81	1.7
’05	3	78	7	2	4	51	26	5	11	0.9	2.9	0.45	2.1
’05	4	49	7	0	–1	38	12	2	6	0.3	1.8	0.09	1.4
’05	5	108	8	2	5	61	25	4	10	0.9	2.9	0.52	2.2
’05	6	97	7	1	3	34	10	2	8	0.3	2.1	0.10	1.4
	MEAN	**87**	**10**	**1**	**5**	**68**	**21**	**4**	**10**	**0.7**	**3.3**	**0.4**	**3.2**

periments conducted in the previous 2 years in the main body of the lake. The mean speeds ranged from 7 to 9 cm s^{-1}, and the U and V magnitudes were more similar because the orientation of the axis of the Inland Sea has a more northeasterly heading compared to the main body of the lake. The MKE ranged from 34 to 60 cm^2 s^{-2}, while the FKE ranged from 10 to 26 cm^2 s^{-2}.

The overall mean statistics for all three years showed an average duration of nearly 4 days (87 h) with a mean speed of 10 cm s^{-1} and a mean U, V of 1 and 5 cm s^{-1}, respectively. The mean speed was nearly twice the mean vector velocity of 5.1 cm s^{-1} $(U^2 + V^2)^{1/2}$ reflecting the oscillatory nature of the flow field. The overall means for MKE and FKE were 68 and 21 cm^2 s^{-2}, respectively. These values were higher than the MKE and FKE values reported by Rao and Murthy (2001) for Lake Ontario. However, their results were based upon sub-surface current meter data that do not resolve the flow in close proximity to the surface.

Simulating Drifter Trajectories

We began our analyses of the drifter data by first using the simplest possible model rather than resort to a complex one to simulate the data. This is a prudent approach regardless of whether the complex model is process driven, stochastic, or heuristic in context. Our model is a simple analytical tool constructed from observed winds. Wind data from Colchester Reef (Fig. 1) were used to build progressive vector diagrams (PVD) using 3% of the wind magnitude as an estimate of the surface current. The PVD has the same start and end time as an individual drifter track that it is being compared to. If the surface currents are dominated by local wind forcing, and the wind field is highly coherent over the space and time span of interest and in the absence of shore constraints, then the wind based PVD and the drifter trajectory should be closely aligned with each other. Figure 5 shows three wind-based PVDs compared against three drifter tracks from 2004 (drifters 1, 4, and 5 in Fig. 5a, b, and c,

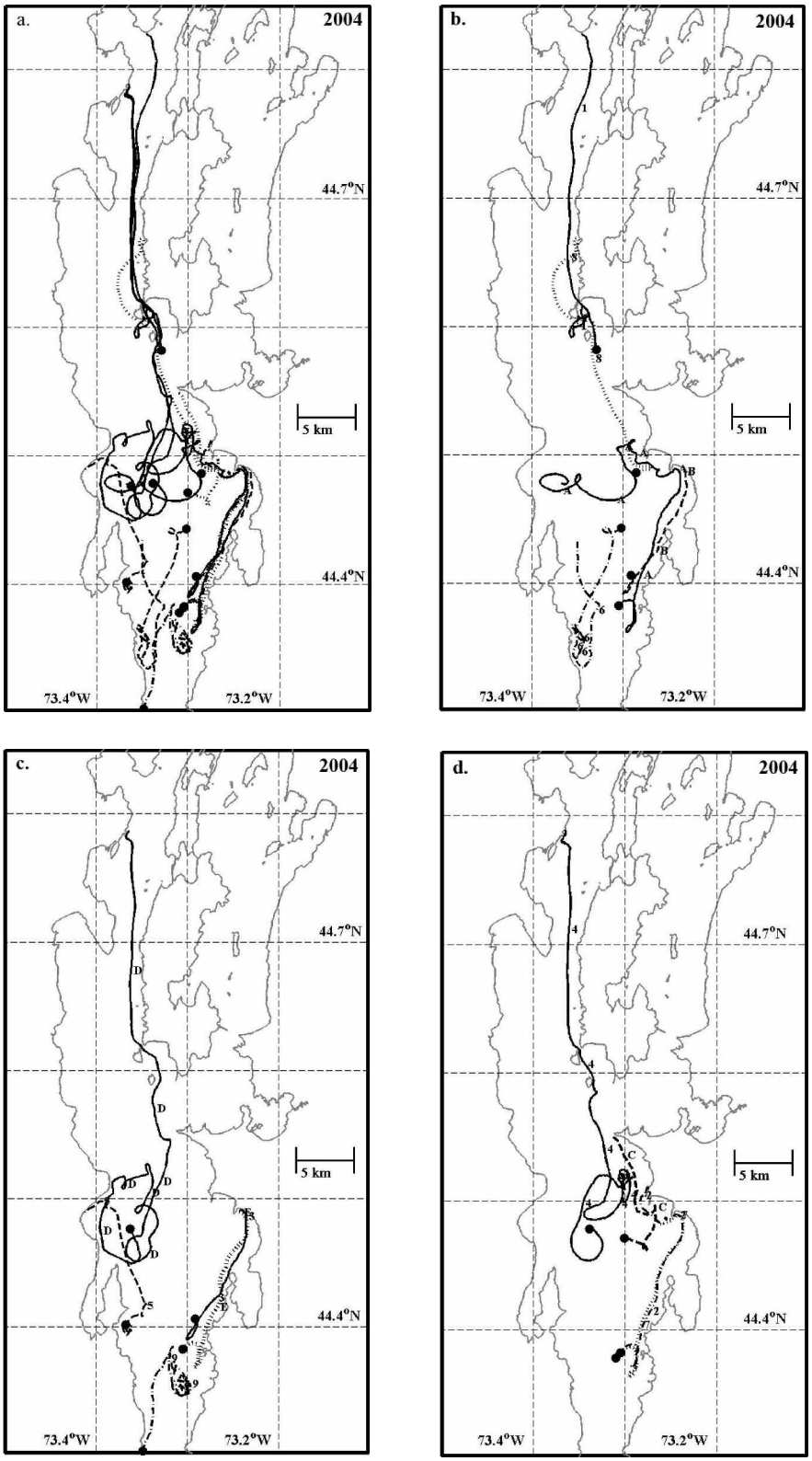

FIG. 3. (a) All tracks for 2004. (b) Tracks 1(—), 6(-.), 8(=), A(—), and B(--). (c) Tracks 3(—), 5(--), 9(-.), D(—) and E(=). (d) Tracks 2(-.), 4(—), 7(=) and C(--). All tracks begin at dark circles, and track symbols repeat every 24 h.

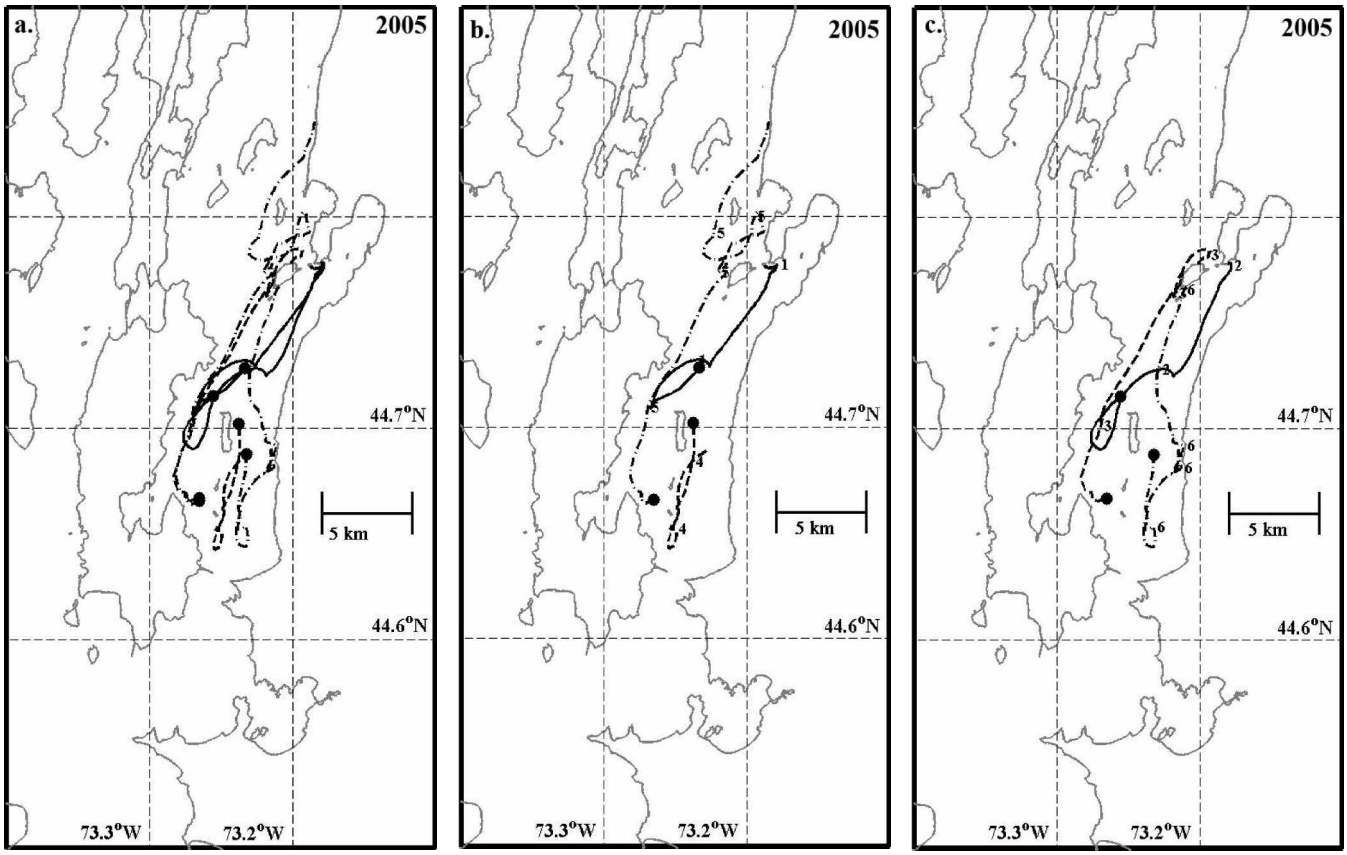

FIG. 4. (a) All tracks for 2005. (b) Tracks 1(—), 4(--), and 5(-.). (c) Tracks 2(—), 3(--) and 6(-.). All tracks begin at dark circles, and track symbols repeat every 24 h.

respectively). In Figure 5a and b, the PVDs qualitatively explain the general drifter trajectory as well as the total drifter displacement. However, in Figure 5c, the drifter trajectory is in opposition to the wind forcing as suggested by the PVD. This is most likely a consequence of the lake-wide circulation whereby a gyre-like circulation is established resulting in upwind transport in the coastal region where drifter 5 was deployed. The other drifter trajectories were in the more open waters of the lake with less impact from shoreline geometry and bottom bathymetry and, therefore, are in better agreement with expectations from direct wind-induced surface currents as suggested by comparison to the PVDs. Examination of the monthly summer wind rose data from Colchester Reef (www.erh.noaa.gov/btv/html/lake.php) from 2003 through 2005 shows winds being predominantly from the S to SSW that is in agreement with the $+V$ predominance of the open water drifter trajectories explained by the 3% PVD model. In general, a wind-based PVD provides a reasonable guess of the surface currents, but it is not as accurate as direct observation or a more comprehensive model of the circulation.

Lagrangian Integral Length and Time Scales and Eddy Diffusivity

The Lagrangian integral time and length scales provide estimates of the decorrelation scales of the surface flow. If a drifter were able to perfectly tag a fluid particle, with no wave or wind induced slippage, then the integral scale calculations are more relevant for estimating the coherence of the flow field. No drifter can completely mimic the behavior of a fluid element, yet the CODE type drifters used here have very low slippage and thus are useful tools for describing various aspects of the surface flow.

All of the following calculations are based upon a Reynolds decomposition of the flow (i.e., $u' = u - U$, $v' = v - V$) to isolate the fluctuating portion of

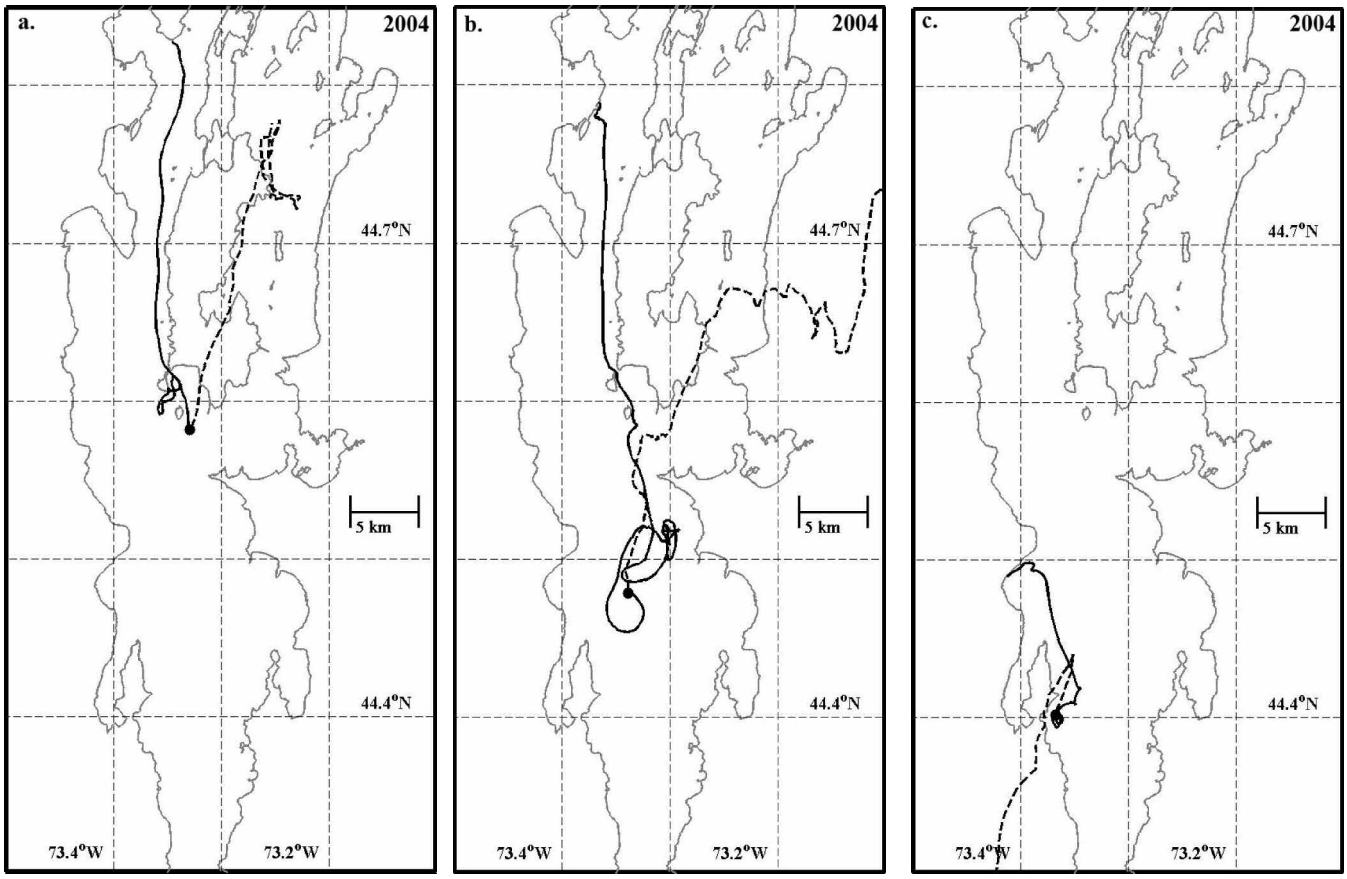

FIG. 5. Progressive vector diagrams comparing 3% of the wind vector (-- lines) against three different drifter tracks (solid lines). Drifter 1 track is in (a), Drifter 4 is in (b), and Drifter 5 is in (c).

the velocity (u', v'). Various authors (e. g., Paduan and Niiler 1993) describe techniques for calculating the Lagrangian statistics that we also include for the sake of completeness. Furthermore, because of the anisotropic nature of the flow, the x and y components of the Lagrangian scales and eddy diffusivity were calculated separately.

The velocity autocorrelation function is the basis from which the decorrelation length and time scales are defined.

$$R_x(\tau) = \frac{\int_0^{(T-\tau)} u'(t)u'(t+\tau)dt}{\int_0^T u'^2(t)dt}, \quad R_y(\tau) = \frac{\int_0^{(T-\tau)} v'(t)v'(t+\tau)dt}{\int_0^T v'^2(t)dt} \quad (4)$$

Equation 4 describes the Lagrangian velocity autocorrelation (R_x, R_y) as a function of the time lag, τ, with T equal to the total time duration that the drifters were afloat. If R_x and R_y are integrated from 0 to the first zero crossing of Equation 4, then the Lagrangian integral time scales (T_x, T_y) are defined as:

$$T_x = \int_0^{T_0} R_x(\tau)d\tau, \quad T_y = \int_0^{T_0} R_y(\tau)d\tau \quad (5)$$

where T_0 is the time of the first zero crossing. The decorrelation times as suggested by the Lagrangian integral time scales ranged from as short as 1 h along the E–W direction (T_x) to as long as 17 h along the N–S direction (T_y). The basin geometry funnels the flow to a preferred orientation along the y-axis resulting in a significantly greater T_y compared to the T_x calculated for the cross-axis flow. The overall T_y for 2003–2005 was 10 h, whereas T_x was only 4 h (Table 2).

The Lagrangian integral length scales (L_x, L_y) were calculated by multiplying the root mean square (rms) of the fluctuating velocity by the right hand sides of Equation 5,

$$L_x = \left[\frac{1}{T}\int_0^T u'^2(t)dt\right]^{1/2} T_x,\ L_y = \left[\frac{1}{T}\int_0^T v'^2(t)dt\right]^{1/2} T_y. \quad (6)$$

The integral length scales showed the same asymmetry in calculated values (Table 2) as was seen in the integral time scales. The cross – axis decorrelation lengths (L_x) were generally less than 1 km with a minimum length of 0.1 km to a maximum of 1.5 km. The primary axis integral length scales (L_y) ranged from a minimum of 1.2 km to a maximum of 8.0 km. The ensemble mean across all years was 0.7 km and 3.3 km for L_x and L_y, respectively.

The Lagrangian eddy diffusivity (K_x, K_y) is based on the theory of single particle diffusivity (Taylor 1921) modified and generalized for both non-isotropic and non-stationary conditions (Davis 1987, Straneo *et al.* 2003). For our applications, the eddy diffusivity was calculated by multiplying the rms fluctuating velocity by the Lagrangian integral length scale:

$$K_x = \left[\left(\frac{1}{T}\int_0^T u'^2(t)dt\right)^{1/2}\right] L_x,\ K_y = \left[\left(\frac{1}{T}\int_0^T v'^2(t)dt\right)^{1/2}\right] L_y. \quad (7)$$

Like the preceding results for the Lagrangian integral time and space scales, the eddy diffusivity results were equally asymmetric in their values as well (Table 2). However, because Equation 7 involves multiplying the integral length scales (Eq. 6) by the rms of (u', v'), it results in approximately an order of magnitude difference between K_x and K_y with K_y being dominant. Analyses of each individual drifter trajectory showed large variations of K_x and K_y with an overall mean of $4 * 10^5$ cm^2 s^{-1} for K_x and $3.2 * 10^6$ cm^2 s^{-1} for K_y.

The Lagrangian statistics calculated for Lake Michigan (McCormick *et al.* 2002) showed similar anisotrophy compared to Lake Champlain with a mean longshore velocity of 3.2 cm s^{-1} and an offshore velocity of 1.3 cm s^{-1}. However, the Lagrangian integral time and length scales were significantly larger than those calculated for Lake Champlain by approximately 3 fold. This is a natural consequence of a physically larger basin's response to surface wind stress generating larger scale circulation patterns. Patterns that translate to greater coherence and thus longer decorrelation scales in coastal regions than would be expected in basins comparable in size to Lake Champlain.

CONCLUSIONS

The mean surface currents of Lake Champlain, as suggested by tracking surface buoys, was approximately 10 cm s^{-1} which is comparable to other large water bodies such as the Great Lakes. Furthermore, the drifter trajectories showed a $+V$ predominance and were qualitatively explained by a 3% PVD model. However, the Lagrangian length and time scales, a measure of flow decorrelation scales, were in general smaller than seen in the Great Lakes, which is a natural consequence of the smaller basin size of Lake Champlain relative to the Great Lakes.

The Lagrangian eddy diffusivities parameterize the turbulence contribution to the mixing of passive tracers, and as such, they often show large variability because of the very nature of turbulence. The values calculated for Lake Champlain (on the order of 10^6 cm^2 s^{-1}) may resemble those for larger lakes and even oceanic regions. Yet, rather than choose a single ensemble mean to represent the eddy diffusivity for Lake Champlain, a spatially dependent eddy diffusivity field may prove to be more useful for advective—diffusive transport modeling applications (Figueroa 1994). Future modeling efforts throughout Lake Champlain and all of its basins may justify the need for such an approach in order to adequately simulate the transport and mixing of passive tracers.

REFERENCES

Davis, R.E. 1985. Drifter observations of coastal surface currents during CODE: the method and descriptive view. *J. Geophys. Res.* 90(C3):4741-4755.

_____. 1987. Modeling eddy transport of passive tracers. *J. Mar. Res.* 45: 635-666.

Figueroa, H.A. 1994. Eddy resolution versus eddy diffusion in a double gyre GCM. Part II: Mixing of Passive Tracers. *J. Phys. Oceanogr.* 24(2):387-402.

Manley, T.O., Hunkins, K.L., Saylor, J.H., Miller, G.S., and Manley, P.L. 1999. Aspects of summertime and wintertime hydrodynamics of Lake Champlain. In *Lake Champlain in transition: From research toward restoration.* T.O. Manley and P.L. Manley, eds., pp. 67-115. Washington, D. C.: American Geophys. Union.

Martin, P.J. 1985. Simulation of the mixed layer at OWS November and Papa with several models. *J. Geophys. Res.* 90:903–916.

McCormick, M.J., and Meadows, G.A. 1988. An intercomparison of four mixed layer models in a shallow inland sea. *J. Geophys. Res.* 93(C6):6774-6788.

_____, Miller, G.S., Murthy, C.R., Rao, Y.R., and Saylor, J.H. 2002. Tracking coastal flow with surface

drifters during the episodic events Great Lakes experiment. *Verh. Internat. Verein. Limnol.* 28:365–369.

_____, Manley, T.O., Foley III, A.J., Gascard, J.C., and Fahnenstiel, G.L. 2006. Lake Champlain Lagrangian experiment. *Verh. Internat. Verein. Limnol.* 29: 1683–1687.

Paduan, J.D., and Niiler, P.P. 1993. Structure of velocity and temperature in the Northeast Pacific as measured with Lagrangian drifters in Fall 1987. *J. Phys. Oceanogr.* 23:585–600.

Rao, Y.R., and Murthy, C.R. 2001. Nearshore currents and turbulent exchange processes during upwelling and downwelling events in Lake Ontario. *J. Geophys. Res.* 106(C2):2667–2678.

Saylor, J.H., Miller, G., Hunkins, K., Manley, T.O., and Manley, P. 1999. Gravity currents and internal bores in Lake Champlain. In *Lake Champlain in transition: From research toward restoration.* T.O. Manley and P.L. Manley, eds., pp. 135–155. Washington, D.C.: American Geophys. Union.

Straneo, F., Pickart, R.S., and Lavender, K. 2003. Spreading of Labrador sea water: an advective-diffusive study based on Lagrangian data. *Deep-Sea Res. Part I.* 50:701–719.

Taylor, G.I. 1921. Diffusion by continuous movements. *Proc. London Math. Soc.* 20:196–212.

Submitted: 31 January 2008
Accepted: 5 August 2008
Editorial handling: Ram R. Yerubandi